Am J Physiol Heart Circ Physiol 325: H1088–H1098, 2023.
First published September 15, 2023; doi:10.1152/ajpheart.00199.2023

american physiological society

AMERICAN JOURNAL OF PHYSIOLOGY
HEART AND CIRCULATORY PHYSIOLOGY

RESEARCH ARTICLE

Energetics and Metabolism

Tissue-specific mitochondrial toxicity of cigarette smoke concentrate: consequence to oxidative phosphorylation

Stephen T. Decker,[1] Alexs A. Matias,[1] Adolfo E. Cuadra,[3] Sean T. Bannon,[1] Jack P. Madden,[1] M. Enes Erol,[1] Corinna Serviente,[1,2] Karine Fenelon,[2,3] and Gwenael Layec[1,2]

[1]*Department of Kinesiology, University of Massachusetts Amherst, Amherst, Massachusetts, United States;* [2]*Institute for Applied Life Science, University of Massachusetts Amherst, Amherst, Massachusetts, United States; and* [3]*Department of Biology, University of Massachusetts Amherst, Amherst, Massachusetts, United States*

Abstract

Cigarette smoke exposure is a well-known risk factor for developing numerous chronic health conditions, including pulmonary disease and cardiometabolic disorders. However, the cellular mechanisms mediating the toxicity of cigarette smoke in extrapulmonary tissues are still poorly understood. Therefore, the purpose of this study was to characterize the acute dose-dependent toxicity of cigarette smoke on mitochondrial metabolism by determining the susceptibility and sensitivity of mitochondrial respiration from murine skeletal (gastrocnemius and soleus) and cardiac muscles, as well as the aorta to cigarette smoke concentrate (CSC). In all tissues, exposure to CSC inhibited tissue-specific respiration capacity, measured by high-resolution respirometry, according to a biphasic pattern. With a break point of 451 ± 235 μg/mL, the aorta was the least susceptible to CSC-induced mitochondrial respiration inhibition compared with the gastrocnemius (151 ± 109 μg/mL; $P = 0.008$, $d = 2.3$), soleus (211 ± 107 μg/mL; $P = 0.112$; $d = 1.7$), and heart (94 ± 51 μg/mL; $P < 0.001$; $d = 2.6$) suggesting an intrinsic resistance of the vascular smooth muscle mitochondria to cigarette smoke toxicity. In contrast, the cardiac muscle was the most susceptible and sensitive to the effects of CSC, demonstrating the greatest decline in tissue-specific respiration with increasing CSC concentration ($P < 0.001$, except the soleus). However, when normalized to citrate synthase activity to account for differences in mitochondrial content, cardiac fibers' sensitivity to cigarette smoke inhibition was no longer significantly different from both fast-twitch gastrocnemius and slow-twitch soleus muscle fibers, thus suggesting similar mitochondrial phenotypes. Collectively, these findings established the acute dose-dependent toxicity of cigarette smoke on oxidative phosphorylation in permeabilized tissues involved in the development of smoke-related cardiometabolic diseases.

NEW & NOTEWORTHY Despite numerous investigations into the mechanisms underlying cigarette smoke-induced mitochondrial dysfunction, no studies have investigated the tissue-specific mitochondrial toxicity to cigarette smoke. We demonstrate that, while aorta is least sensitive and susceptible to cigarette smoke-induced toxicity, the degree of cigarette smoke-induced toxicity in striated muscle depends on the tissue-specific mitochondrial content. We conclude that while the mitochondrial content influences cigarette smoke-induced toxicity in striated muscles, aorta is intrinsically protected against cigarette smoke-induced mitochondrial toxicity.

aorta; cardiac muscle; cigarette smoke; high-resolution respirometry; skeletal muscle

INTRODUCTION

Cigarette smoke exposure is a well-known and significant health concern in the United States, contributing to 480,000 premature deaths and costing an estimated $300 billion annually in direct and indirect costs (1). Chronic cigarette smoking has a causative role in the development of respiratory diseases. In addition, mounting evidence indicates a dose-dependent increase in the risks for cardiovascular and metabolic diseases, skeletal muscle atrophy and weakness, or frailty in smokers (2–5). Despite the strong epidemiological link between cigarette smoking and numerous adverse health outcomes, the exact cellular mechanisms mediating the toxicity of cigarette smoke on tissues throughout the body are still poorly understood.

Mitochondria are the major energy source of most organs in humans and are also involved in maintaining cellular redox balance, calcium homeostasis, and apoptosis. Expanding on the central role of mitochondria in maintaining homeostasis in a wide range of cell types, a growing number of studies

Correspondence: G. Layec (glayec@umass.edu).
Submitted 10 April 2023 / Revised 11 September 2023 / Accepted 12 September 2023

suggest that mitochondria may be implicated as a mediator of the multisystemic defects induced by cigarette smoke exposure. Mainstream cigarette smoke is composed of over 4,800 different chemicals, including reactive oxygen species (ROS) and toxins (6), which can impair mitochondrial function (7, 8). Specifically, acute exposure to reactive oxygen species lowered the activity of several Krebs cycle enzymes and maximal respiration in isolated mitochondria (9). Also, direct exposure to cigarette smoke compounds, nicotine and *o*-cresol, inhibited maximal respiration in isolated mitochondria in vitro (10). Although these findings were essential as proof of concept that cigarette smoke exposure can alter mitochondrial function, the use of isolated mitochondria in these studies is an important caveat, as this approach exaggerates mitochondrial susceptibility to dysfunction (11), which limited the translational impact of these findings.

In lung epithelial cells, it is well described that acute exposure to cigarette smoke condensate elicits substantial bioenergetics perturbation and redox stress. Specifically, mitochondrial membrane potential and ATP production are lowered by exposure to cigarette smoke concentrate (CSC) as a result of the modulation of the mitochondrial ADP/ATP transporter thus increasing proton leak (7, 12–14). These energetic perturbations are accompanied by greater mitochondrial-derived ROS generation (12–14) and increased susceptibility to apoptosis (15). In contrast, the mitochondrial toxicity of cigarette smoke on other organs or tissues has been scarcely investigated. For instance, acute exposure to cigarette smoke or nicotine, a constituent of tobacco, resulted in lower proton driving force and increased mitochondrial-derived ROS production in cultured cardiomyocytes (16) and carotid arteries (17, 18).

A major caveat with these studies was that the cigarette smoke concentrations used (upward of 20% of the total solution) in those preparations was well above the physiological range of cigarette smoke particulate found in the blood of smokers (19, 20), making the findings from these studies challenging to translate to in vivo conditions in humans. Also, although the organs' susceptibility to the harmful effects of cigarette smoke differs, as illustrated by the greater relative risks for disease in some tissues (3, 21), the tissue-dependent toxicity of cigarette smoke on mitochondrial function remains unknown.

Therefore, this study aimed to characterize the toxicity of acute exposure to cigarette smoke concentrate on mitochondrial respiratory capacity in permeabilized tissues from cardiac, skeletal, and smooth muscles, as this approach closely replicates mitochondrial functional properties in vivo (7, 22–24). Based on prior epidemiological studies demonstrating an exaggerated cardiovascular disease burden compared with other chronic diseases in smokers (3), we hypothesized that cardiac and smooth muscle tissues would be more susceptible (lower break point from piecewise linear regression analysis) and sensitive (steeper slope after the break point) to cigarette smoke concentrate-induced mitochondrial toxicity than fast- and slow-twitch skeletal muscles.

METHODS

Animals and Experimental Design

Mature male and female C57BL/6 mice (mean age, 31 ± 12 wk) were used for this study. All animals were maintained on a 12-h:12-h dark/light cycle without access to running wheels and were fed standard chow ad libitum. Following euthanasia by 5% isoflurane, the gastrocnemius, soleus, left ventricle, and aorta were extracted and placed in ice-cold BIOPS preservation solution. The gastrocnemius and soleus were specifically chosen because of the similarities in mitochondrial respiratory rates per unit of mass compared with those of human vastus lateralis muscle (24), and to encompass tissues that contain varying amounts of type I and type II skeletal muscle (25). Animal use and husbandry followed protocols approved by the University of Massachusetts Institutional Animal Care and Use Committee (IACUC No. 2152).

Cigarette Smoke Concentrate Preparation

Cigarette smoke concentrate (Murty Pharmaceuticals, Lexington, KY) containing 40 mg of cigarette smoke particulate matter/mL (henceforth considered 100%) was diluted in MiR05, consisting of (in mM) 110 sucrose, 0.5 EGTA, 3 $MgCl_2$, 60 K-lactobionate, 20 taurine, 10 KH_2PO_4, and 20 HEPES, and 1 g/L BSA at pH 7.1, to obtain six different concentrations of cigarette smoke concentrate ranging from 0.004 (0.00001%) to 2,400 μg/mL (6%) before being stored at −80°C.

Citrate Synthase Activity

In a separate cohort of mice ($n = 7$, mean age, 20 ± 10 wk), tissues (gastrocnemius, soleus, heart, and aorta) were harvested as described earlier and then immediately placed in 2 mL of MiR-05 and incubated for 20 min. Each sample was snap frozen in liquid nitrogen after incubation and stored at −80°C for later analysis. Tissues were thawed and homogenized on ice in a buffer containing 1 mM EDTA and 50 mM triethanolamine, as previously described (11). Samples were transferred to a 96-well plate containing 200 μM acetyl-CoA, 200 μM DTNB, and 70 μM oxaloacetate, where spectrophotometric analysis of citrate synthase activity was assessed using a multimode reader (Synergy HTX BioTek Instruments, Winooski, VT) by detecting the increase in absorbance at 412 nm at 30°C (11).

Preparation of Permeabilized Tissues and Mitochondrial Respiration Measurements

The tissue preparation and respiration measurement techniques were adapted from established methods (23, 26) and have been previously described by our group (27). Briefly, BIOPS-immersed fibers (in mM: 2.77 CaK_2EGTA, 7.23 K_2EGTA, 50 K^+ MES, 6.56 $MgCl_2$, 20 taurine, 5.77 ATP, 15 PCr, 0.5 DTT, and 20 imidazole) were carefully separated with fine-tip forceps and subsequently bathed in a BIOPS-based saponin solution (50 μg saponin/mL BIOPS) for 30 min for the gastrocnemius, soleus, and heart and 40 min for the aorta as previously described (28, 29). Following saponin treatment, tissues were rinsed twice in ice-cold mitochondrial respiration fluid (MIR05, in mM: 110 sucrose, 0.5 EGTA, 3 $MgCl_2$, 60 K-lactobionate, 20 taurine, 10 KH_2PO_4, and 20 HEPES, and 1 g/L BSA at pH 7.1) for 10 min each. After the muscle sample was gently dabbed with a paper towel to remove excess fluid, the wet weight of the sample (1 to 2 mg) was measured using a standard, calibrated scale. The muscle fibers were then placed in the respiration chamber (Oxygraph O2K, Oroboros Instruments, Innsbruck, Austria) with 2 mL of MIR05 solution warmed to 37°C. Oxygen was

added to the chambers, and oxygen concentration was maintained between 175 and 250 μM for the gastrocnemius, soleus, and aorta and between 350 and 450 μM for the right ventricle. After we allowed the permeabilized muscle sample to equilibrate for 5 min, mitochondrial respiratory function was assessed in duplicate. To determine maximal ADP-stimulated respiration (state III with convergent electron flow from complex I and II), glutamate (10 mM), malate (2 mM), ADP (5 mM), and succinate (10 mM) were added to the chamber (GMDS). Cytochrome-*c* (10 μM) was then added to the chamber to assess mitochondrial membrane integrity. Samples that demonstrated impaired mitochondrial membrane integrity (more than a 10% increase in respiration in response to cytochrome-*c*) were excluded from the analysis (23, 26). Following the test for membrane integrity, cigarette smoke concentrate was injected into each chamber at incremental concentrations starting from 0.004 (0.00001%) up to 2,400 μg/mL (6%). In each condition, the respiration rate was recorded until a steady state of at least 30 s (at a sampling rate of 2 s) was reached, the average of which was used for data analysis. The rate of O_2 consumption was expressed relative to muscle sample mass (in pmol O_2/s/mg wet wt), or normalized to citrate synthase activity (in pmol O_2/s per CS) to determine tissue-specific and mitochondria-specific respiration, respectively.

Data Analysis

The assessment of the normality and homoscedasticity was performed using a Shapiro–Wilk and Levene test for all the variables. The effects of cigarette smoke concentrate on mitochondrial respiration were determined using a nonparametric two-way (tissue × concentration) aligned ranks transform (ART) ANOVA (30). Planned comparisons of the effect of cigarette smoke concentrations on state III respiration (GMDS), as established a priori, were determined using Dunn's tests with a Holm–Šidák adjustment.

A piecewise linear regression model based on the logarithmic transformation ($\log_{10}$) of the concentration of cigarette smoke concentrate was used to estimate break points in the dose-dependent changes to mitochondrial respiration. The break point and the slope after the break point were used to determine the susceptibility and sensitivity, respectively, of a given tissue to cigarette smoke toxicity, respectively. To adjust the $\log_{10}$ transform for concentrations at 0 ($\log_{10}(0)$ = infinity), 0.0004 was added to all concentrations such that the log-transformed values for each concentration of cigarette smoke concentrate (x) was equal to $\log_{10}(x + 0.0004)$. The differences between each tissue on break point, slope, and IC_{50} were determined using a nonparametric Kruskal–Wallis test, followed by post hoc pairwise Dunn's test with a Holm–Šidák adjustment. Statistical significance was accepted at $P \leq 0.05$. All statistical analyses were performed using R, version 4.1. Break-point analyses were performed using the "segmented" (31) package. Dose-response curves using a three-parameter Weibull-type two dose-response functions in the "drc" package were used to estimate the IC_{50} and are shown in the Supplemental Figs. S1 and S2 (all Supplemental Figures are available at https://doi.org/10.6084/m9.figshare.c.6855297). Effect sizes (Cohen's d) were calculated using the "emmeans" package. Results are presented as means ± SD in text and means ± SE in figures.

RESULTS

Tissue-Specific Citrate Synthase Activities

Citrate synthase activities, used as markers of mitochondrial content, for each tissue are shown in Fig. 1. There was a significant main effect of tissue type on the citrate synthase activity ($P < 0.001$; $\eta^2 = 0.94$). Post hoc analyses indicated that citrate synthase activity in the heart (63.8 ± 6.4 AU) was significantly higher than the soleus (22.3 ± 5.4 AU; $P < 0.001$, $d = 6.4$), gastrocnemius (9.4 ± 3.4 AU; $P < 0.001$, $d = 8.4$), and aorta (36.4 ± 9.3 AU; $P = 0.025$, $d = 4.3$).

Effects of Cigarette Smoke Concentrate on Tissue-Specific Rates of Respiration

Tissue-specific respiration rates are shown in Fig. 2. There were significant main effects of cigarette smoke concentrate ($P < 0.001$; partial $\eta^2 = 0.72$) and tissue type ($P < 0.001$; partial $\eta^2 = 0.72$), as well as a significant interaction effect ($P < 0.001$; partial $\eta^2 = 0.33$). Post hoc analyses for each tissue (Fig. 3) indicated that the respiration rates of the gastrocnemius, soleus, and heart were significantly (adjusted $P < 0.05$) inhibited by cigarette smoke starting at

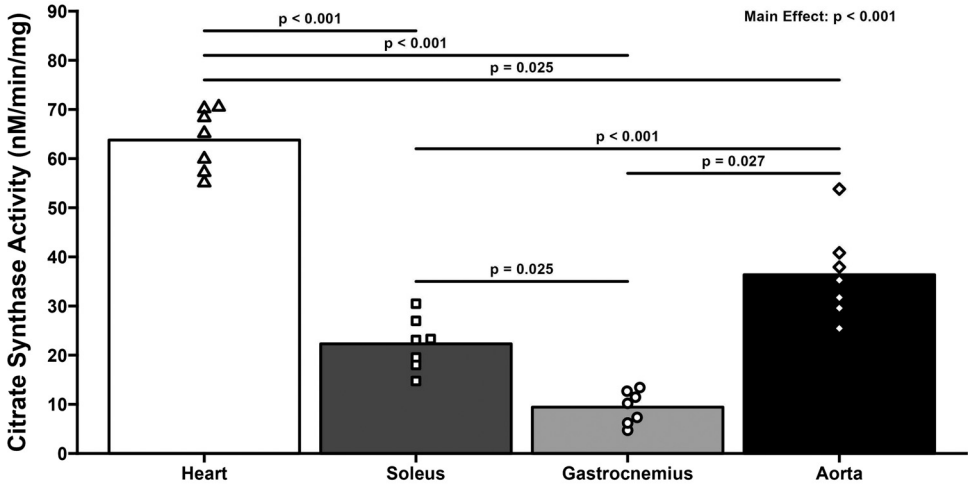

Figure 1. Citrate synthase activity for the heart (white), soleus (dark gray), gastrocnemius (light gray), and aorta (black). n = 7 for all tissues. Values are represented as means ± SE.

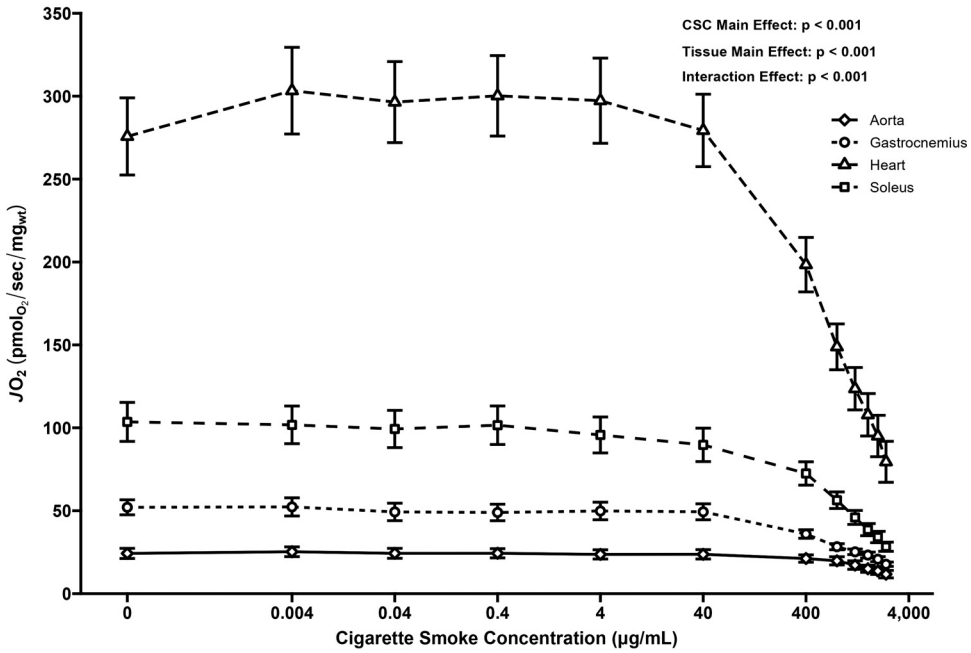

Figure 2. Relationship between cigarette smoke concentrate (CSC) concentration and tissue-specific respiration rates for the heart (n = 9; triangles), soleus (n = 11; squares), gastrocnemius (n = 11; circles), and aorta (n = 8; diamonds). Values are represented as means ± SE.

800 μg/mL (2%), 800 μg/mL (2%), and 1,200 μg/mL (3%), respectively. The cigarette smoke-induced decrements to mitochondrial respiration trended toward significance ($P = 0.054$) at the highest concentration of cigarette smoke used in this study (2,400 μg/mL, 6%)

Results of the piecewise linear regression are shown in Fig. 4. Results from the one-way ANOVA indicated a significant main effect of tissue type on the break point at which cigarette smoke concentrate inhibited mitochondrial respiration ($P = 0.001$; $\eta^2 = 0.40$; Fig. 4*A*). Based on the post hoc analysis, the concentration of cigarette smoke concentrate at which the break point occurred in the aorta (450.9 ± 235.3 μg/mL) was significantly different from the heart (93.6 ± 50.6 μg/mL; $P = 0.001$; $d = 2.6$) and the gastrocnemius (150.9 ± 108.6 μg/mL; $P = 0.005$, $d = 2.2$), but not the soleus (211.0 ± 108.0 μg/mL; $P = 0.081$; $d = 0.7$). Likewise, there was a significant difference between the heart and soleus ($P = 0.031$; $d = 0.9$). However, there were no significant differences between the soleus and the gastrocnemius ($P = 0.170$; $d = 0.4$), nor were there differences between the gastrocnemius and the heart ($P = 0.123$; $d = 0.4$).

Likewise, tissue type had a significant main effect on the slope following the break ($P < 0.001$; $\eta^2 = 0.84$; Fig. 4*B*). Post hoc analyses indicated that the rate of cigarette smoke concentrate-induced inhibition in the heart (−145.1 ± 45.5 JO_2/cigarette smoke concentrate) was significantly different from the gastrocnemius (−22.0 ± 7.8 JO_2/cigarette smoke concentrate; $P < 0.001$, $d = 4.8$) and aorta (−15.1 ± 8.9 JO_2/cigarette smoke concentrate; $P < 0.001$, $d = 5.1$), and trended in the soleus (−55.5 ± 22.7 JO_2/cigarette smoke concentrate; $P = 0.053$, $d = 3.5$). Likewise, the rate of cigarette smoke concentrate-induced inhibition in the soleus was significantly different from the gastrocnemius ($P = 0.015$, $d = 1.3$) and the aorta ($P = 0.002$, $d = 1.6$). However, there was not a significant difference between the rate of cigarette smoke concentrate-induced inhibition in the gastrocnemius and the aorta ($P = 0.161$, $d = 0.3$).

Effects of Cigarette Smoke Concentrate on Mitochondria-Specific Respiration across Tissues

Mitochondrial respiration rates normalized to citrate synthase activity are shown in Fig. 5. There were significant main effects of cigarette smoke concentrate ($P < 0.001$; partial $\eta^2 = 0.72$) and tissue type ($P < 0.001$; partial $\eta^2 = 0.72$), as well as a significant interaction effect ($P < 0.001$; partial $\eta^2 = 0.33$). Post hoc analyses for each tissue (Fig. 5, *A*–*D*) indicated that the normalized respiration rates of the gastrocnemius, soleus, heart, and aorta were significantly (adjusted $P < 0.05$) inhibited by cigarette smoke concentrate starting at 400, 800, 1,200, and 2,400 μg/mL, respectively.

Results of the piecewise linear regression are shown in Fig. 6. Results from the one-way ANOVA indicated a significant main effect of tissue type on the break point at which cigarette smoke concentrate impaired mitochondrial respiration ($P = 0.001$; $\eta^2 = 0.40$; Fig. 6*A*). Post hoc analysis revealed that the cigarette smoke concentrate at which the break point occurred in the aorta (450.9 ± 235.2 μg/mL) was significantly higher than the heart (93.6 ± 50.6 μg/mL; $P < 0.001$; $d = 2.6$) and the gastrocnemius (150.9 ± 108.6 μg/mL; $P = 0.008$, $d = 2.3$), but not the soleus (211.0 ± 107.0 μg/mL; $P = 0.112$; $d = 1.7$). There were also significant differences between the soleus and heart ($P = 0.031$; $d = 0.9$). However, there were no significant differences between the soleus and the gastrocnemius ($P = 0.170$; $d = 0.4$); nor were there differences between the gastrocnemius and the heart ($P = 0.128$; $d = 0.4$).

Likewise, tissue type had a significant main effect on the slope following the break ($P < 0.001$; $\eta^2 = 0.53$; Fig. 6*B*). Post hoc analyses indicated that the rate of cigarette smoke concentrate-induced inhibition in the aorta (−0.8 ± 0.4 JO_2/citrate synthase/cigarette smoke concentrate) was significantly lower than the heart (−2.6 ± 1.4 JO_2/citrate synthase/cigarette smoke concentrate; $P = 0.022$, $d = 1.6$), soleus (−3.4 ± 0.9 JO_2/CS/cigarette smoke concentrate; $P < 0.001$, $d = 2.3$), and gastrocnemius (−3.9 ± 1.5 JO_2/citrate synthase/cigarette smoke

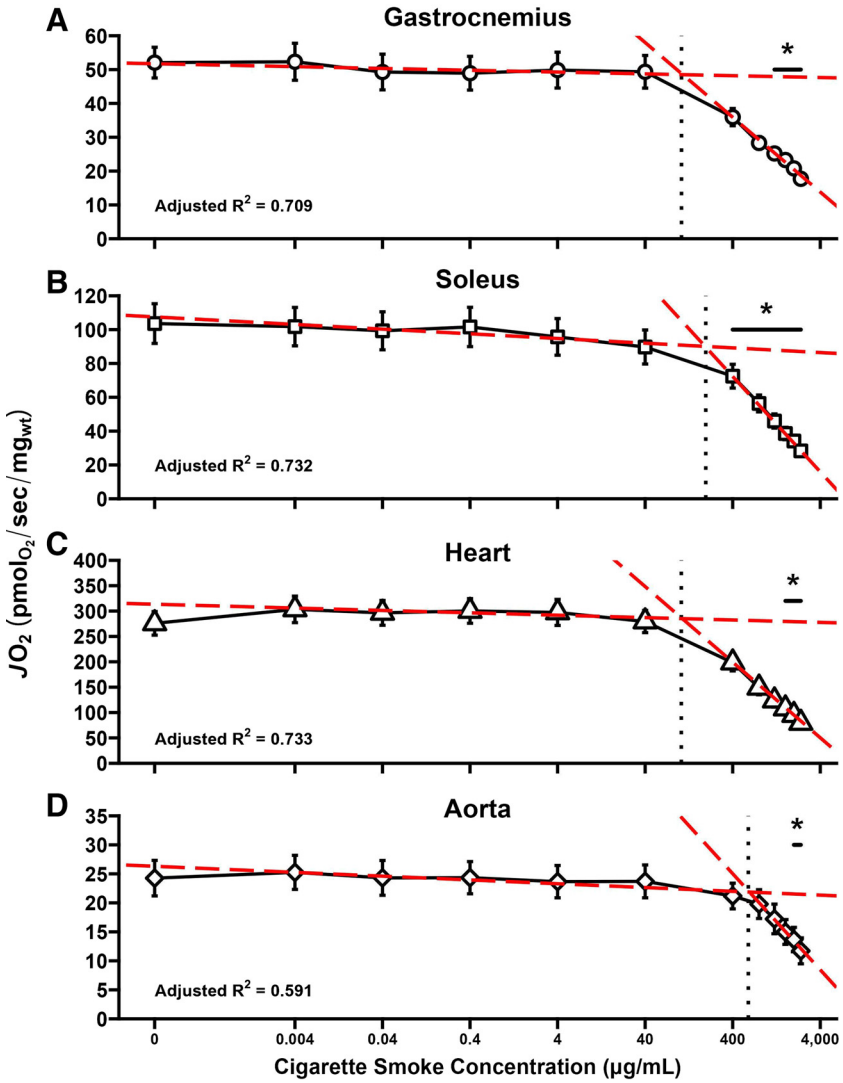

Figure 3. Relationship between cigarette smoke concentrate concentration and tissue-specific respiration rates for the gastrocnemius ($n = 11$; *A*), soleus ($n = 11$; *B*), heart ($n = 9$; *C*), and aorta ($n = 8$; *D*) fitted with a piecewise linear regression. Break points are indicated by the dotted black line. Slopes of the piecewise linear regression are indicated by the red dashed lines. Values are represented as means ± SE. *$P < 0.05$, significantly different from glutamate, malate, ADP, and succinate (GMDS, 0 µg/mL) following post hoc analysis using Dunn's test with a Holm–Sidak correction.

concentrate; $P < 0.001$, $d = 2.7$). However, there were no significant differences between the heart and the gastrocnemius ($P = 0.132$, $d = 1.1$) or the soleus ($P = 0.181$, $d = 0.7$); nor were there significant differences between the gastrocnemius and the soleus ($P = 0.347$, $d = 0.4$).

DISCUSSION

Mitochondrial dysfunction has been implicated as a potential mediator of the cardiometabolic dysregulation associated with cigarette smoking. Accordingly, this study aimed to characterize the toxicity of acute exposure to cigarette smoke concentrate on mitochondrial respiratory capacity in permeabilized tissues from cardiac, skeletal, and smooth muscles. Exposure to cigarette smoke concentrate inhibited mitochondrial respiration capacity consistent with a biphasic pattern in all tissues. Furthermore, the differences in break points and slopes after the break point revealed both tissue-specific susceptibility and sensitivity to cigarette smoke.

Specifically, cardiac tissues exhibited the greatest susceptibility and the greatest sensitivity to cigarette smoke concentrate toxicity, whereas the aorta was the least sensitive and least susceptible. When normalized to citrate synthase activity to account for differences in mitochondrial content, cardiac fibers' sensitivity to cigarette smoke inhibition was no longer significantly different from both fast-twitch gastrocnemius and slow-twitch soleus muscle fibers, thus suggesting similar mitochondrial phenotypes. In contrast, even after normalization for mitochondrial content, the aorta remained the least susceptible and least sensitive to cigarette smoke-induced inhibition of mitochondrial respiration, suggesting an intrinsic resistance of the vascular smooth muscle mitochondria to cigarette smoke toxicity. This characterization of the dose-effect of cigarette smoke concentrate on skeletal, cardiac, and smooth muscle tissues on mitochondrial respiration capacity indicates that, compared with striated muscles, vascular smooth muscle has intrinsic characteristics that provide greater protection from smoke-induced mitochondrial toxicity.

Cigarette Smoke Concentrate Directly Inhibits Tissue-Specific Respiration

The dose-response of cigarette smoke concentrate on tissue-specific respiration rates were characteristics of a

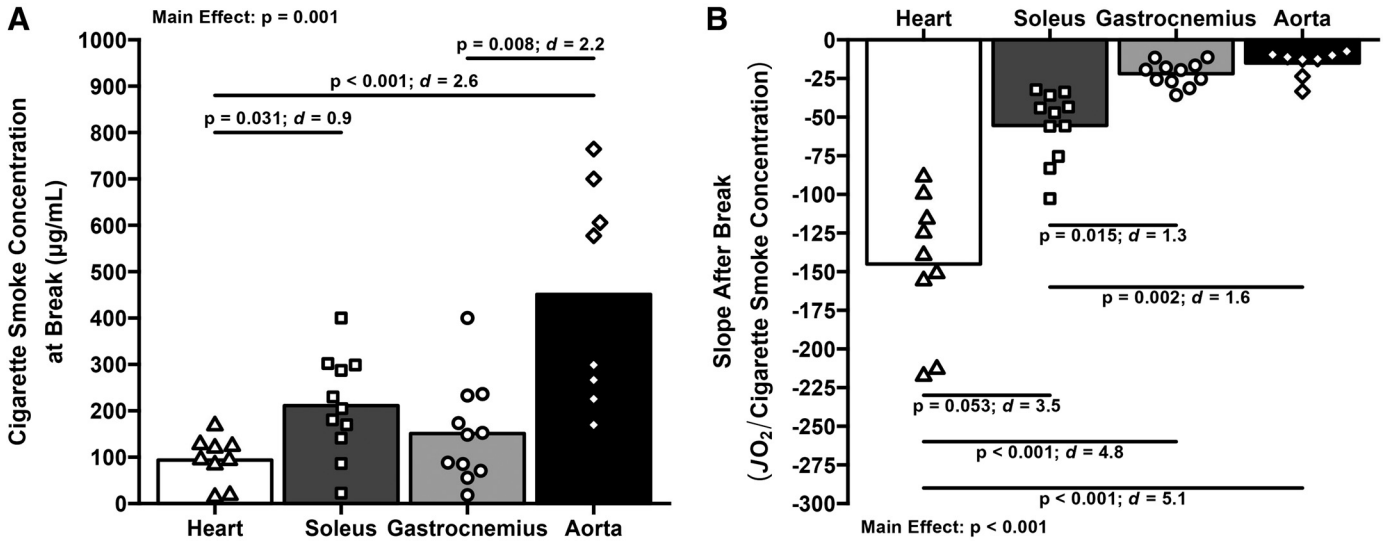

Figure 4. Parameters estimates from the piecewise linear regression of the relationship between cigarette smoke concentrate concentration and tissue-specific respiration rates. Estimates of the break point (*A*) and the slope following the breaking point (*B*) for the heart ($n = 9$; white), soleus ($n = 11$; dark gray), gastrocnemius ($n = 11$; light gray), and aorta ($n = 8$; black). Values are represented as means ± SE.

threshold model as beyond a concentration of 200–500 µg/mL (~0.5–1%), cigarette smoke concentrate had an evident dose-dependent inhibitory effect on mitochondrial respiration in all tissues, as shown in Figs. 2 and 3. Moreover, at the final concentration of 2,400 µg/mL (6%) cigarette smoke concentrate, maximal ADP-stimulated respirations with convergent electron flow from complex I and II were inhibited by as much as ~60% in the striated muscles (gastrocnemius, soleus, and heart), and by ~40% in the smooth muscles from the aorta. The toxicity of cigarette smoke concentrate on tissue-specific respiration observed in the present study was consistent with the derangements of mitochondrial function previously documented in a range of tissues, including lung epithelial tissue, carotid arteries, cardiac muscle, and skeletal muscle. (10, 12, 14, 17, 32–35). Notably, the present study extends these findings obtained in vitro to intact permeabilized tissues in situ. The use of permeabilized tissues has indeed the added benefit of maintaining the structural integrity of the surrounding cellular environment, which, considering that mitochondria form a reticulum across cells (36), preserves the mitochondrial structure (11), and better reflects the functional characteristics of the mitochondria in vivo (22–24).

These methodological differences between the use of isolated mitochondria and permeabilized fibers have important implications in regard to the susceptibility to cigarette smoke concentrate toxicity. For example, Khattri et al. (10) found that incubating mitochondria isolated from a mixture of mouse skeletal muscles in 0.02, 0.1, and 1.0% cigarette smoke concentrate solution for 10 min impaired maximal ADP-stimulated respiration by 5, 22, and 61%, respectively. In contrast, the present study provides evidence that permeabilized cardiac and skeletal muscle fibers are more resistant to cigarette smoke concentrate than mitochondria isolated from skeletal muscle, as much higher (~2–10 times) cigarette smoke concentrate concentrations were needed to elicit decrements in mitochondrial respiration of similar magnitude. Therefore, although cigarette smoke concentrate-induced toxicity was evident in both preparations, there are distinct differences in the concentration of cigarette smoke concentrate required to cause acute mitochondrial metabolic dysfunction between isolated mitochondria and intact tissue samples. Such differences have an important bearing on the conclusion when translating these findings to determine the functional effects of smoking at clinically relevant levels.

A strength of the present study was the use of concentrations for the dose response that encompassed both physiological and supraphysiological amounts of cigarette smoke to characterize toxicity on mitochondrial metabolism. Based on prior studies indicating that in vivo levels of water-soluble components of cigarette smoke in the plasma from smokers corresponded to cigarette smoke concentrations <40 µg/mL or 0.1% (17, 19, 20, 32, 37), our results indicate that cigarette smoke concentrate demonstrated no significant effect on mitochondrial respiration in permeabilized tissues at clinically relevant concentration. Specifically, the dose-response analysis identified a break point of 200–500 µg/mL (0.5–1%), beyond which cigarette smoke concentrate inhibited mitochondrial respiration in striated and smooth muscles. This threshold is, therefore, five to 10 times higher than plasmatic levels of water-soluble components of cigarette smoke in the plasma from smokers (37), which seems to rule out a direct inhibitory effect of cigarette smoke concentrate, at least acutely, on mitochondrial respiratory capacity in striated and smooth muscles in vivo. Previous studies using various preparation in vitro had reported a linear dose-dependent decrease in mitochondrial respiration exposed to cigarette smoke concentrate (14, 38). However, these studies relied on supraphysiological concentrations of cigarette smoke concentrate (>1%) to characterize the effects of cigarette smoke concentrate on mitochondrial respiration. Therefore, our findings build on these results to demonstrate that acute cigarette smoke concentrate exposure at clinically relevant concentrations appears to have a limited effect on oxidative phosphorylation capacity in tissues, yet, highly

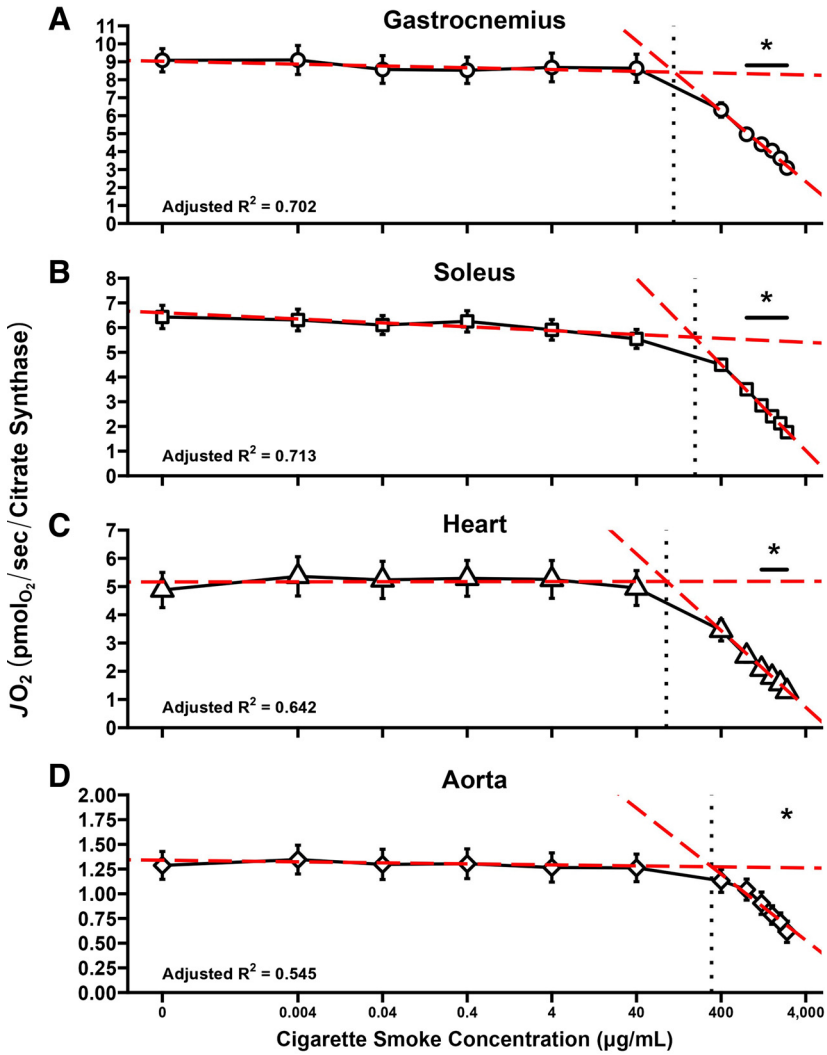

Figure 5. Relationship between cigarette smoke concentrate (cigarette smoke concentrate) concentration and mitochondrial-specific respiration rate for the gastrocnemius ($n = 11$; *A*), soleus ($n = 11$; *B*), heart ($n = 9$; *C*), and aorta ($n = 8$; *D*) fitted with a piecewise linear regression. Red dashed lines indicate the two slopes calculated from the piecewise linear regression, with the estimated break point represented as the black dotted line. Citrate synthase activity was used a marker of mitochondrial content. Values are expressed as means ± SE. *$P < 0.05$, significantly different from glutamate, malate, ADP, and succinate (GMDS, 0 µg/mL) following post hoc analysis using Dunn's test with a Holm–Sidak correction.

susceptible to smoke-related diseases. Interestingly, previous studies in mouse models of second-hand cigarette smoke documented rather subtle effects of chronic exposure to cigarette smoke on skeletal muscle respiratory capacity whereas mitochondrial oxidative stress was evident (39, 40). Based on these findings, alterations in the cellular redox state via increased mitochondrial superoxide generation may be of importance in regulating the cigarette smoke-induced loss of mitochondrial respiration. Although these outcomes were not measured in the present study, it is possible that cigarette smoke exposure causes an increase in mitochondrial electron leak and superoxide generation, thereby directly decreasing electron flux through the electron transport chain (ETC) and oxygen consumption at the site of complex IV. Future studies are therefore warranted to examine whether changes in mitochondrial ROS generation, rather than energy production, underlie the metabolic anomalies and the development of cardiometabolic diseases associated with smoking. Moreover, studies examining the abilities of mitochondria-target ROS scavengers, such as MitoQ (41) or Mito-TEMPO (42), to rescue cigarette smoke-induced mitochondrial dysfunction are also warranted.

Mitochondria from Aortic Smooth Muscles Are Less Susceptible and Sensitive to Cigarette Smoke Concentrate than Striated Muscles

A central aim of the present study was to characterize the susceptibility and sensitivity to cigarette smoke concentrate of the aorta, cardiac, and two metabolically distinct skeletal muscle fibers. Using a piecewise linear regression, we identified a break point at which cigarette smoke significantly started to inhibit mitochondrial respiration (Fig. 4*A*). Based on this rigorous analysis, we estimate that the mitochondria in the smooth muscles of the aorta exhibited deficits in mitochondrial respiration beginning at ~500 µg/mL cigarette smoke concentrate—i.e., between two and five times the amount of cigarette smoke concentrate required to inhibit respiration in the gastrocnemius, soleus, and cardiac muscle fibers. This difference remained even after accounting for mitochondrial content by normalizing the data to citrate synthase activity (Fig. 6*A*). Moreover, the sensitivity (Fig. 4*B*) of the smooth muscles of the aorta to cigarette smoke concentrate-induced inhibition of mitochondrial respiration was the lowest of the tissues used in the present study by two- to five-fold, especially when normalized for citrate synthase activity

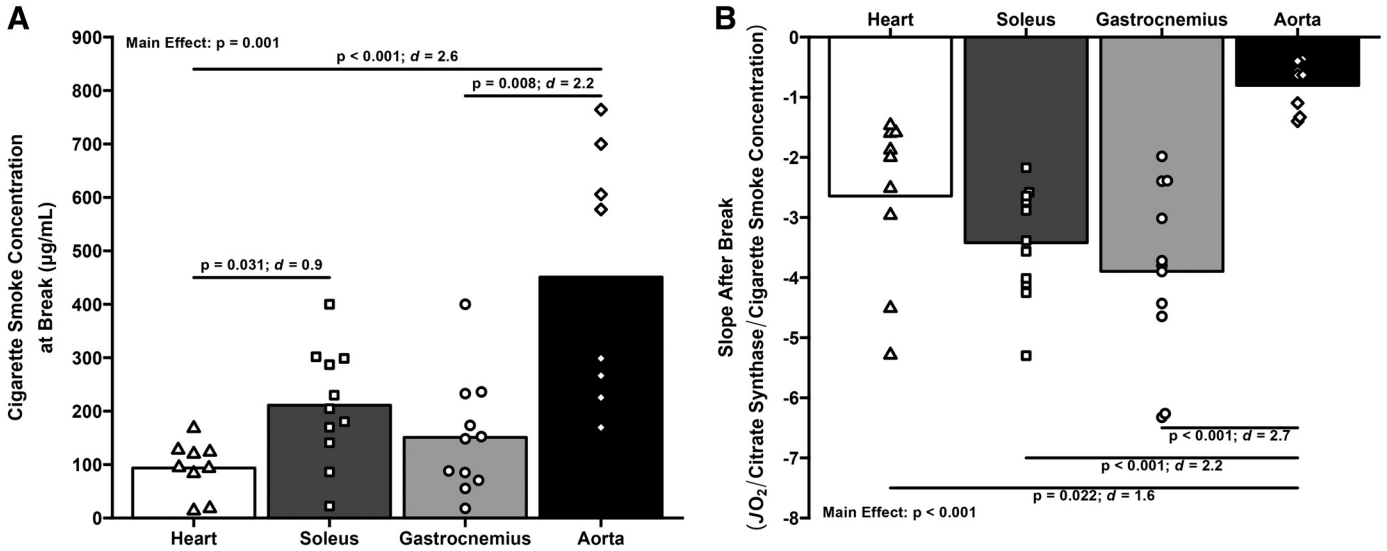

Figure 6. Parameters estimates from the piecewise linear regression of the relationship between cigarette smoke concentrate concentration and mitochondrial-specific respiration rates. Estimates of the break point (*A*) and the slope following the breaking point (*B*) for the heart ($n = 9$; white), soleus ($n = 11$; dark gray), gastrocnemius ($n = 11$; light gray), and aorta ($n = 8$; black). Values are expressed as means ± SE. *P* values are adjusted for multiple comparisons using Dunn's test with a Holm–Sidak correction.

(Fig. 6*B*). Our estimation of the concentration of CSC at 50% of maximal respiration was also in agreement with these data (Supplemental Fig. S2). We also estimated the dose-response curves for these experiments that are in agreement with these data (Supplemental Fig. S1); however, we caution the interpretation of these data because of our inability to achieve a lower limit of cigarette smoke-induced inhibition on mitochondrial respiration. Nonetheless, we provide evidence that the mitochondria in the aorta are intrinsically less susceptible to the negative impacts of cigarette smoke exposure than mitochondria in skeletal and cardiac muscles.

This finding of different intrinsic mitochondrial resistance to stressors such as cigarette smoke is unique, as mitochondria from cardiac muscle, skeletal muscle, and skeletal muscle feed arteries have been shown to have similar respiration rates when these tissues are normalized for differences in mitochondrial content, as measured by citrate synthase activity (43). In addition, much like skeletal muscle, mitochondria in the feed arteries or aorta have been shown to respond positively to exercise training (29) and impaired with advancing age (28), suggesting metabolic similarities between mitochondria in the vasculature and skeletal muscle. However, the citrate synthase activities of the skeletal muscle feed arteries in these studies were much lower than the citrate synthase activity reported here. Although we cannot fully explain the discrepancies between our results and the other studies, it is possible that there are inherent differences in the mitochondrial content across the vascular tree. Furthermore, considering the wide diversity of the structural and functional components of vascular tissues (44), it is possible that there are, likewise, very distinct morphological properties of the mitochondria across the vascular tree. Specifically, it is widely considered that the main role of peripheral arteries, such as skeletal muscle feed arteries, is to regulate local blood flow and maintain mean arterial pressure, whereas the role of more centrally located arteries, such as the aorta, is to withstand the extremely high pressure invoked by systolic contractions of the heart (44). As such, to maintain arterial compliance in response to large variations in pressure, central arteries are composed of tissues that maintain arterial stiffness (i.e., elastin, collagen), which become less abundant in peripheral arteries (44). These changes in artery composition may play important roles in shaping the morphology of the mitochondrial reticulum (45) in the specific regions of the vascular tree, thus altering the regional function of the mitochondria. However, further research is needed to determine the structural properties of mitochondria across the vascular network.

Respiration Sensitivity to Cigarette Smoke Concentrate in Striated Muscle is Dependent on Mitochondrial Content

In contrast to the relative resistance to cigarette smoke concentrate observed in the aorta, the cardiac and soleus muscle fibers were much more sensitive to cigarette smoke concentrate-induced inhibition of mitochondrial respiratory capacity than the gastrocnemius muscle. As such, the cardiac muscle fibers exhibited a loss of mitochondrial respiration per unit of cigarette smoke concentrate at a rate three times greater than the soleus and six times greater than the gastrocnemius. Similarly, the respiration rate of the soleus muscle fibers decreased at a rate two times greater than the gastrocnemius. However, these significant findings were abolished when the cigarette smoke concentrate-induced decreases in respiration rates were normalized to mitochondrial content measured by citrate synthase activity. Therefore, these findings suggest that the differences in sensitivity between striated muscles can predominantly be attributed to the differences in mitochondrial content of these tissues rather than some other inherent property of the mitochondria within those tissues.

Although the break point for cigarette smoke concentrate-induced inhibition of mitochondrial respiration was beyond the plasmatic concentration measured in smokers, our results are consistent with the hypothesis that cardiac muscles and oxidative type I fibers may be more vulnerable to the deleterious

effects of cigarette smoke. Chronic smoking is indeed associated with dramatic increases in numerous chronic cardiovascular and muscular ailments, including peripheral artery disease, heart failure, type II diabetes, and sarcopenia (2–5, 46). The mitochondrial density-dependent inhibition induced by cigarette smoke concentrate in striated muscles in the present study may explain, in part, the high incidence of cardiomyopathies in chronic smokers (i.e., heart failure) and why type I muscle fibers are more apt to atrophy and contractile dysfunction than type II fibers in chronic smokers (47–49). Ventricular remodeling is a common manifestation in several models of smoke exposure in animals (50) and humans (51–53). Given the greater mitochondrial density of the left ventricle and the soleus (~6- and ~2-fold greater than the gastrocnemius), these tissues would likely be more prone to cigarette smoke concentrate-induced deficits in mitochondrial bioenergetics due to their greater reliance on oxidative ATP production. The bioenergetic deficits in the soleus muscles could also activate cellular mechanisms, which result in muscle atrophy (54) as often reported in chronic smokers (55). Together, these findings suggest that tissues with a greater mitochondrial density may be more sensitive to cigarette smoke toxicity and dysfunction, perhaps, due to their greater reliance on oxidative energy supply. In this scenario, the decrements in mitochondrial function may result in a mismatch between ATP supply and demand that, ultimately, leads to loss of cellular function and poor health outcomes.

Conclusions

In conclusion, this study rigorously characterized the sensitivity and susceptibility characteristics of cigarette smoke-induced mitochondrial dysfunction in skeletal (slow and fast-twitch), cardiac, and smooth muscles. Collectively, the results from this study suggest that inherent characteristics of mitochondria in the aorta increase its resistance to cigarette smoke metabolic toxicity. On the other hand, cigarette smoke concentrate inhibition of mitochondrial respiration in striated muscles was dependent on the mitochondrial density, with tissues rich in mitochondria (cardiac and slow-twitch fibers) demonstrated greater sensitivity and susceptibility to the perturbations in mitochondrial metabolism induced by cigarette smoke. However, considering the range of bioenergetic demand in these tissues, especially cardiac muscle, even minor deficits in oxidative ATP production could rapidly lead to bioenergetic failure and organ dysfunction. Thus, the findings in the present study established cigarette smoke dose-response on mitochondrial oxidative phosphorylation in permeabilized tissues linked to cigarette smoke adverse health outcomes thus contributing to our understanding of the cellular mechanisms involved in the development of smoke-related cardiometabolic diseases.

DATA AVAILABILITY

Data are available upon reasonable request from corresponding author.

SUPPLEMENTAL DATA

Supplemental Figs. S1 and S2: https://doi.org/10.6084/m9.figshare.c.6855297.

GRANTS

This work was funded in part by National Heart, Lung, and Blood Institute Grant R00HL125756 (to G.L.).

DISCLOSURES

No conflicts of interest, financial or otherwise, are declared by the authors.

AUTHOR CONTRIBUTIONS

S.T.D., J.P.M., C.S., K.F., and G.L. conceived and designed research; S.T.D., A.A.M., A.E.C., S.T.B., J.P.M. and M.E.E. performed experiments; S.T.D., A.A.M., S.T.B., J.P.M., and M.E.E. analyzed data; S.T.D., S.T.B., M.E.E., C.S., and G.L. interpreted results of experiments; S.T.D. prepared figures; S.T.D. drafted manuscript; S.T.D., A.A.M., A.E.C., S.T.B., J.P.M., M.E.E., C.S., K.F., and G.L. edited and revised manuscript; S.T.D., A.A.M., A.E.C., S.T.B., J.P.M., M.E.E., C.S., K.F., and G.L. approved final version of manuscript.

REFERENCES

1. **United States Department of Health and Human Services.** *The Health Consequences of Smoking—50 Years of Progress*. Atlanta, GA: Centers for Disease Control and Prevention (US), 2014.
2. **Maddatu J**, **Anderson-Baucum E**, **Evans-Molina C.** Smoking and the risk of type 2 diabetes. *Transl Res* 184: 101–107, 2017. doi:10.1016/J.TRSL.2017.02.004.
3. **Münzel T**, **Hahad O**, **Kuntic M**, **Keaney JF**, **Deanfield JE**, **Daiber A.** Effects of tobacco cigarettes, e-cigarettes, and waterpipe smoking on endothelial function and clinical outcomes. *Eur Heart J* 41: 4057–4070, 2020. doi:10.1093/EURHEARTJ/EHAA460.
4. **Jo Y**, **Linton JA**, **Choi J**, **Moon J**, **Kim J**, **Lee J**, **Oh S.** Association between cigarette smoking and sarcopenia according to obesity in the middle-aged and elderly Korean population: the Korea National Health and Nutrition Examination Survey (2008–2011). *Korean J Fam Med* 40: 87–92, 2019. doi:10.4082/KJFM.17.0078.
5. **Lee N**, **Choi CJ.** Smoking and diabetes as predictive factors of accelerated loss of muscle mass in middle-aged and older women: a six-year retrospective cohort study. *J Womens Health (Larchmt)* 28: 1391–1398, 2019. doi:10.1089/JWH.2018.7527.
6. **Rodgman A**, **Green C.** Toxic chemicals in cigarette mainstream smoke—hazard and hoopla. *Int/Contrib Tobacco Res* 20: 481–545, 2014. doi:10.2478/cttr-2013-0764.
7. **Decker ST**, **Alexandrou-Majaj N**, **Layec G.** Effects of acute cigarette smoke concentrate exposure on mitochondrial energy transfer in fast- and slow-twitch skeletal muscle. *Biochim Biophys Acta Bioenerg* 1864: 148973, 2023. doi:10.1016/j.bbabio.2023.148973.
8. **Decker ST**, **Matias AA**, **Bannon ST**, **Madden JP**, **Alexandrou-Majaj N**, **Layec G.** Effects of cigarette smoke on in situ mitochondrial substrate oxidation of slow- and fast-twitch skeletal muscles. *Life Sci* 315: 121376, 2023. doi:10.1016/J.LFS.2023.121376.
9. **Nulton-Persson AC**, **Szweda LI.** Modulation of mitochondrial function by hydrogen peroxide. *J Biol Chem* 276: 23357–23361, 2001. doi:10.1074/JBC.M100320200.
10. **Khattri RB**, **Thome T**, **Fitzgerald LF**, **Wohlgemuth SE**, **Hepple RT**, **Ryan TE.** NMR spectroscopy identifies chemicals in cigarette smoke condensate that impair skeletal muscle mitochondrial function. *Toxics* 10: 140, 2022. doi:10.3390/TOXICS10030140.
11. **Picard M**, **Ritchie D**, **Wright KJ**, **Romestaing C**, **Thomas MM**, **Rowan SL**, **Taivassalo T**, **Hepple RT.** Mitochondrial functional impairment with aging is exaggerated in isolated mitochondria compared to permeabilized myofibers. *Aging Cell* 9: 1032–1046, 2010. doi:10.1111/j.1474-9726.2010.00628.x.
12. **Van Der Toorn M**, **Rezayat D**, **Kauffman HF**, **Bakker SJL**, **Gans ROB**, **Koëter GH**, **Choi AMK**, **Van Oosterhout AJM**, **Slebos DJ.** Lipid-soluble components in cigarette smoke induce mitochondrial production of reactive oxygen species in lung epithelial cells. *Am J Physiol Lung Cell Mol Physiol* 297: L109–L114, 2009. doi:10.1152/ajplung.90461.2008.

13. **Wu K**, **Luan G**, **Xu Y**, **Shen S**, **Qian S**, **Zhu Z**, **Zhang X**, **Yin S**, **Ye J.** Cigarette smoke extract increases mitochondrial membrane permeability through activation of adenine nucleotide translocator (ANT) in lung epithelial cells. *Biochem Biophys Res Commun* 525: 733–739, 2020 [Erratum in *Biochem Biophys Res Commun* 533: 1527–1528, 2020]. doi:10.1016/j.bbrc.2020.02.160.
14. **Van Der Toorn M**, **Slebos DJ**, **De Bruin HG**, **Leuvenink HG**, **Bakker SJL**, **Gans ROB**, **Koëter GH**, **Van Oosterhout AJM**, **Kauffman HF.** Cigarette smoke-induced blockade of the mitochondrial respiratory chain switches lung epithelial cell apoptosis into necrosis. *Am J Physiol Lung Cell Mol Physiol* 292: L1211–L1218, 2007. doi:10.1152/ajplung.00291.2006.
15. **Aoshiba K**, **Tamaoki J**, **Nagai A.** Acute cigarette smoke exposure induces apoptosis of alveolar macrophages. *Am J Physiol Lung Cell Mol Physiol* 281: L1392–L1401, 2001. doi:10.1152/AJPLUNG.2001.281.6.L1392.
16. **Jia G**, **Meng Z**, **Liu C**, **Ma X**, **Gao J**, **Liu J**, **Guo R**, **Yan Z**, **Christopher T**, **Lopez B**, **Liu W**, **Dai H**, **Lau WB**, **Jiao X**, **Zhao J**, **Wang ZX**, **Cao J**, **Wang Y.** Nicotine induces cardiac toxicity through blocking mitophagic clearance in young adult rat. *Life Sci* 257: 118084, 2020. doi:10.1016/J.LFS.2020.118084.
17. **Orosz Z**, **Csiszar A**, **Labinskyy N**, **Smith K**, **Kaminski PM**, **Ferdinandy P**, **Wolin MS**, **Rivera A**, **Ungvari Z.** Cigarette smoke-induced proinflammatory alterations in the endothelial phenotype: role of NAD(P)H oxidase activation. *Am J Physiol Heart Circ Physiol* 292: H130–H139, 2007. doi:10.1152/ajpheart.00599.2006.
18. **Csiszar A**, **Labinskyy N**, **Podlutsky A**, **Kaminski PM**, **Wolin MS**, **Zhang C**, **Mukhopadhyay P**, **Pacher P**, **Hu F**, **De Cabo R**, **Ballabh P**, **Ungvari Z.** Vasoprotective effects of resveratrol and SIRT1: attenuation of cigarette smoke-induced oxidative stress and proinflammatory phenotypic alterations. *Am J Physiol Heart Circ Physiol* 294: H2721–H2735, 2008. doi:10.1152/ajpheart.00235.2008.
19. **Mendelson JH**, **Sholar MB**, **Mutschler NH**, **Jaszyna-Gasior M**, **Goletiani NV**, **Siegel AJ**, **Mello NK.** Effects of intravenous cocaine and cigarette smoking on luteinizing hormone, testosterone, and prolactin in men. *J Pharmacol Exp Ther* 307: 339–348, 2003. doi:10.1124/jpet.103.052928.
20. **Benowitz NL**, **Kuyt F**, **Jacob P.** Circadian blood nicotine concentrations during cigarette smoking. *Clin Pharmacol Ther* 32: 758–764, 1982. doi:10.1038/CLPT.1982.233.
21. **Gandini S**, **Botteri E**, **Iodice S**, **Boniol M**, **Lowenfels AB**, **Maisonneuve P**, **Boyle P.** Tobacco smoking and cancer: a meta-analysis. *Int J Cancer* 122: 155–164, 2008. doi:10.1002/IJC.23033.
22. **Layec G**, **Gifford JR**, **Trinity JD**, **Hart CR**, **Garten RS**, **Park SY**, **Le Fur Y**, **Jeong EK**, **Richardson RS.** Accuracy and precision of quantitative 31P-MRS measurements of human skeletal muscle mitochondrial function. *Am J Physiol Endocrinol Physiol* 311: E358–E366, 2016. doi:10.1152/ajpendo.00028.2016.
23. **Kuznetsov AV**, **Veksler V**, **Gellerich FN**, **Saks V**, **Margreiter R**, **Kunz WS.** Analysis of mitochondrial function in situ in permeabilized muscle fibers, tissues and cells. *Nat Protoc* 3: 965–976, 2008. doi:10.1038/nprot.2008.61.
24. **Jacobs RA**, **Díaz V**, **Meinild AK**, **Gassmann M**, **Lundby C.** The C57Bl/6 mouse serves as a suitable model of human skeletal muscle mitochondrial function. *Exp Physiol* 98: 908–921, 2013. doi:10.1113/expphysiol.2012.070037.
25. **Augusto V**, **Padovani CR**, **Campos GER.** Skeletal muscle fiber types in C57BL6J mice. *Braz J Morphol Sci* 21: 89–94, 2004.
26. **Pesta D**, **Gnaiger E.** High-resolution respirometry: OXPHOS protocols for human cells and permeabilized fibers from small biopsies of human muscle. *Methods Mol Biol* 810: 25–58, 2012. doi:10.1007/978-1-61779-382-0_3.
27. **Layec G**, **Blain GM**, **Rossman MJ**, **Park SY**, **Hart CR**, **Trinity JD**, **Gifford JR**, **Sidhu SK**, **Weavil JC**, **Hureau TJ**, **Amann M**, **Richardson RS.** Acute high-intensity exercise impairs skeletal muscle respiratory capacity. *Med Sci Sports Exerc* 50: 2409–2417, 2018. doi:10.1249/MSS.0000000000001735.
28. **Park SH**, **Park SY**, **Kwon OS**, **Park SHSY**, **Weavil JC**, **Andtbacka RHI**, **Hyngstrom JR**, **Reese V**, **Richardson RS.** Vascular mitochondrial respiratory function: the impact of advancing age. *Am J Physiol Heart Circ Physiol* 315: H1660–H1669, 2018. doi:10.1152/ajpheart.00324.2018.
29. **Park SY**, **Rossman MJ**, **Gifford JR**, **Bharath LP**, **Bauersachs J**, **Richardson RS**, **Abel ED**, **Symons JD**, **Riehle C.** Exercise training improves vascular mitochondrial function. *Am J Physiol Heart Circ Physiol* 310: H821–H829, 2016. doi:10.1152/ajpheart.00751.2015.
30. **Wobbrock JO**, **Findlater L**, **Gergle D**, **Higgins JJ.** The aligned rank transform for nonparametric factorial analyses using only ANOVA procedures. In: *Conference on Human Factors in Computing Systems—Proceedings*. New York: ACM Press, 2011, p. 143–146. doi:10.1145/1978942.1978963.
31. **Muggeo V.** Segmented: An R Package to Fit Regression Models With Broken-Line Relationships (Online). R News. 2008. https://www.researchgate.net/publication/234092680_Segmented_An_R_Package_to_Fit_Regression_Models_With_Broken-Line_Relationships [2022 Apr 18].
32. **Csiszar A**, **Podlutsky A**, **Wolin MS**, **Losonczy G**, **Pacher P**, **Ungvari Z.** Oxidative stress and accelerated vascular aging: implications for cigarette smoking. *Front Biosci* 14: 3128–3144, 2009. doi:10.2741/3440.
33. **Naserzadeh P**, **Pourahmad J.** Toxicity mechanisms of cigarette smoke on eye and kidney using isolated mitochondria. *Iran J Pharm Sci* 9: 55–62, 2013.
34. **Naserzadeh P**, **Hosseini M-J**, **Arbabi S**, **Pourahmad J.** A comparison of toxicity mechanisms of cigarette smoke on isolated mitochondria obtained from rat liver and skin. *Iran J Pharm Res* 14: 271–277, 2015.
35. **Thatcher MO**, **Tippetts TS**, **Nelson MB**, **Swensen AC**, **Winden DR**, **Hansen ME**, **Anderson MC**, **Johnson IE**, **Porter JP**, **Reynolds PR**, **Bikman BT.** Ceramides mediate cigarette smoke-induced metabolic disruption in mice. *Am J Physiol Endocrinol Physiol* 307: E919–E927, 2014. doi:10.1152/ajpendo.00258.2014.
36. **Glancy B**, **Hartnell LM**, **Malide D**, **Yu ZX**, **Combs CA**, **Connelly PS**, **Subramaniam S**, **Balaban RS.** Mitochondrial reticulum for cellular energy distribution in muscle. *Nature* 523: 617–620, 2015. doi:10.1038/nature14614.
37. **Gourlay SG**, **Benowitz NL.** Arteriovenous differences in plasma concentration of nicotine and catecholamines and related cardiovascular effects after smoking, nicotine nasal spray, and intravenous nicotine. *Clin Pharmacol Ther* 62: 453–463, 1997. doi:10.1016/S0009-9236(97)90124-7.
38. **Ajime TT**, **Serré J**, **Wüst RCI**, **Messa GAM**, **Poffé C**, **Swaminathan A**, **Maes K**, **Janssens W**, **Troosters T**, **Degens H**, **Gayan-Ramirez G.** Two weeks of smoking cessation reverse cigarette smoke-induced skeletal muscle atrophy and mitochondrial dysfunction in mice. *Nicotine Tob Res* 23: 143–151, 2021. doi:10.1093/ntr/ntaa016.
39. **Kwon OS**, **Decker ST**, **Zhao J**, **Hoidal JR**, **Heuckstadt T**, **Sanders KA**, **Richardson RS**, **Layec G.** The receptor for advanced glycation end products (RAGE) is involved in mitochondrial function and cigarette smoke-induced oxidative stress. *Free Radic Biol Med* 195: 261–269, 2023. doi:10.1016/J.FREERADBIOMED.2022.12.089.
40. **Decker ST**, **Kwon OS**, **Zhao J**, **Hoidal JR**, **Huecksteadt TP**, **Richardson RS**, **Sanders KA**, **Layec G**, **Heuckstadt T**, **Sanders KA**, **Richardson RS**, **Layec G.** Skeletal muscle mitochondrial adaptations induced by long-term cigarette smoke exposure. *Am J Physiol Endocrinol Physiol* 321: E80–E89, 2021. doi:10.1152/ajpendo.00544.2020.
41. **Kelso GF**, **Porteous CM**, **Coulter CV**, **Hughes G**, **Porteous WK**, **Ledgerwood EC**, **Smith RAJ**, **Murphy MP.** Selective targeting of a redox-active ubiquinone to mitochondria within cells: antioxidant and antiapoptotic properties. *J Biol Chem* 276: 4588–4596, 2001. doi:10.1074/JBC.M009093200.
42. **Trnka J**, **Blaikie FH**, **Smith RAJ**, **Murphy MP.** A mitochondria-targeted nitroxide is reduced to its hydroxylamine by ubiquinol in mitochondria. *Free Radic Biol Med* 44: 1406–1419, 2008. doi:10.1016/J.FREERADBIOMED.2007.12.036.
43. **Park SY**, **Gifford JR**, **Andtbacka RHI**, **Trinity JD**, **Hyngstrom JR**, **Garten RS**, **Diakos NA**, **Ives SJ**, **Dela F**, **Larsen S**, **Drakos S**, **Richardson RS.** Cardiac, skeletal, and smooth muscle mitochondrial respiration: are all mitochondria created equal? *Am J Physiol Heart Circ Physiol* 307: H346–H352, 2014. doi:10.1152/ajpheart.00227.2014.
44. **Lacolley P**, **Regnault V**, **Segers P**, **Laurent S.** Vascular smooth muscle cells and arterial stiffening: relevance in development, aging, and disease. *Physiol Rev* 97: 1555–1617, 2017. doi:10.1152/PHYSREV.00003.2017.
45. **Glancy B**, **Hartnell LM**, **Combs CA**, **Femnou A**, **Sun J**, **Murphy E**, **Subramaniam S**, **Balaban RS.** Power grid protection of the muscle

mitochondrial reticulum. *Cell Rep* 19: 487–496, 2017 [Erratum in *Cell Rep* 23: 2832, 2018]. doi:10.1016/J.CELREP.2017.03.063.

46. **Steffl M**, **Bohannon RW**, **Petr M**, **Kohlikova E**, **Holmerova I.** Relation between cigarette smoking and sarcopenia: meta-analysis. *Physiol Res* 64: 419–426, 2015. doi:10.33549/physiolres.932802.
47. **Gosker HR**, **Langen RC**, **Bracke KR**, **Joos GF**, **Brusselle GG**, **Steele C**, **Ward KA**, **Wouters EF**, **Schols AM.** Extrapulmonary manifestations of chronic obstructive pulmonary disease in a mouse model of chronic cigarette smoke exposure. *Am J Respir Cell Mol Biol* 40: 710–716, 2009. doi:10.1165/rcmb.2008-0312OC.
48. **Gosker HR**, **Zeegers MP**, **Wouters EF**, **Schols AM.** Muscle fibre type shifting in the vastus lateralis of patients with COPD is associated with disease severity: a systematic review and meta-analysis. *Thorax* 62: 944–949, 2007. doi:10.1136/thx.2007.078980.
49. **Degens H**, **Gayan-Ramirez G**, **Van Hees HW.** Smoking-induced skeletal muscle dysfunction: from evidence to mechanisms. *Am J Respir Crit Care Med* 191: 620–625, 2015. doi:10.1164/rccm.201410-1830PP.
50. **Kaplan A**, **Abidi E**, **Ghali R**, **Booz GW**, **Kobeissy F**, **Zouein FA.** Functional, cellular, and molecular remodeling of the heart under influence of oxidative cigarette tobacco smoke. *Oxid Med Cell Longev* 2017: 3759186, 2017. doi:10.1155/2017/3759186.
51. **Barutcu I**, **Esen AM**, **Kaya D**, **Onrat E**, **Melek M**, **Celik A**, **Kilit C**, **Turkmen M**, **Karakaya O**, **Esen OB**, **Saglam M**, **Kirma C.** Effect of acute cigarette smoking on left and right ventricle filling parameters: a conventional and tissue Doppler echocardiographic study in healthy participants. *Angiology* 59: 312–316, 2008. doi:10.1177/0003319707304882.
52. **Minicucci MF**, **Azevedo PS**, **Polegato BF**, **Paiva SA**, **Zornoff LA.** Cardiac remodeling induced by smoking: concepts, relevance, and potential mechanisms. *Inflamm Allergy Drug Targets* 11: 442–447, 2012. doi:10.2174/187152812803589958.
53. **Nadruz W**, **Claggett B**, **Gonçalves A**, **Querejeta-Roca G**, **Fernandes-Silva MM**, **Shah AM**, **Cheng S**, **Tanaka H**, **Heiss G**, **Kitzman DW**, **Solomon SD.** Smoking and cardiac structure and function in the elderly: the ARIC Study (Atherosclerosis Risk in Communities). *Circ Cardiovasc Imaging* 9: e004950, 2016. doi:10.1161/CIRCIMAGING.116.004950.
54. **Hyatt H**, **Deminice R**, **Yoshihara T**, **Powers SK.** Mitochondrial dysfunction induces muscle atrophy during prolonged inactivity: a review of the causes and effects. *Arch Biochem Biophys* 662: 49–60, 2019. doi:10.1016/J.ABB.2018.11.005.
55. **Montes De Oca M**, **Loeb E**, **Torres SH**, **De Sanctis J**, **Hernández N**, **Tálamo C.** Peripheral muscle alterations in non-COPD smokers. *Chest* 133: 13–18, 2008. doi:10.1378/chest.07-1592.